BIOCHEMISTRY
including biophysical chemistry & molecular biology

Article

pubs.acs.org/biochemistry

Interaction of *Saccharomyces cerevisiae* HMO2 Domains with Distorted DNA

Sreerupa Ray† and Anne Grove*

Department of Biological Sciences, Louisiana State University, Baton Rouge, Louisiana 70803, United States

Supporting Information

ABSTRACT: The *Saccharomyces cerevisiae* high mobility group protein HMO2 is a component of the chromatin remodeling complex INO80. In this capacity, it has been shown to direct INO80 to DNA double-strand breaks, thereby contributing to double-strand break repair. Consistent with such function, HMO2 binds DNA ends, protecting them from exonucleolytic degradation. We show here that both domains of HMO2, HMO2-BoxA and HMO2-BoxB, bind preferentially to distorted DNA, with HMO2-BoxA binding preferentially to four-way DNA junctions and DNA with tandem mismatches and HMO2-BoxB binding four-way junctions as well as DNA with stem−loop structures, tandem mismatches, and abasic sites. As previously reported for mammalian high mobility group proteins, the acidic C-terminal extension significantly attenuates DNA binding. Notably, the unique ability of HMO2 to protect DNA ends is conferred by the Box A domain. Considering the reported roles for INO80 in other events such as recovery of stalled replication forks and nucleotide excision repair, we assessed the effect of DNA damaging agents on an *hmo2*Δ strain; while modest growth inhibition is seen upon exposure to UV light, exposure to hydroxyurea, which causes replication fork arrest, induces severe growth deficiency. These data suggest that HMO2 may also participate in directing the INO80 complex to sites such as stalled replication forks; the preferred binding of HMO2 domains to damaged DNA and intermediates in homologous recombination is consistent with such function.

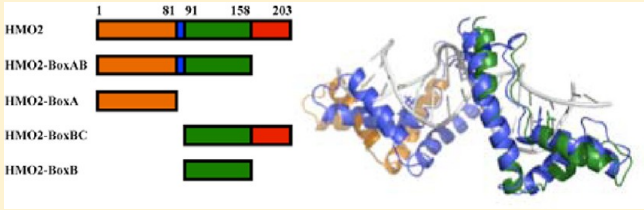

High mobility group (HMGB) proteins are architectural proteins found ubiquitously in eukaryotes where they play varied roles in DNA-dependent processes such as DNA recombination, transcription, and repair.[1−6] HMGB proteins usually contain two DNA-binding HMG domains, named Box A and Box B, followed by an acidic C-terminal tail, and they bind to DNA in a non-sequence specific manner. Each HMG box is composed of ∼80 amino acids, which adopt an L-shaped fold created from three α-helices, and DNA binding occurs through the minor groove of the DNA by partial intercalation of hydrophobic amino acid residues.[7−11] As for other DNA-bending proteins, binding to DNA with noncanonical structures is energetically favorable, and HMGB proteins bind preferentially to distorted DNA such as cis-platin [*cis*-diaminedichloroplatinum(II)]-modified DNA and four-way junctions.[12,13]

Of several HMGB proteins in *Saccharomyces cerevisiae*, HMO1 and HMO2 (also known as NHP10) contain a Box B domain that resembles that of mammalian HMGB proteins and a Box A domain with only limited similarity. For HMO1, Box B contributes primarily to DNA binding affinity, the Box A domain is necessary for bending of duplex DNA, and the unique lysine-rich C-terminal tail mediates in-phase DNA bending.[14−16] Numerous functions for HMO1 have been reported, including roles in rDNA transcription and coordination of ribosomal protein and rRNA production in response to signaling by the target of the rapamycin (TOR) pathway (reviewed in ref 17). In contrast, the only reported function of HMO2 is its role in directing the INO80 chromatin remodeling complex to double-strand breaks (DSBs).[18−21] Recently, we reported that HMO2 binds to DNA ends and protects them from exonuclease III digestion, consistent with a role in DSB repair.[22]

In addition to functions in DNA double-strand break repair, INO80 has also been implicated in nucleotide excision repair, specifically the repair of UV photoproducts, and in the restart of stalled replication forks.[23−26] Under these circumstances, noncanonical DNA structures are formed. DSBs, UV lesions, and replication stress result in the phosphorylation of histone H2A on serine 129 to generate γ-H2AX, an event shown to be important for INO80 recruitment.[19,20,27−29] Considering that HMO2 binds DNA ends, one substrate to which INO80 is recruited, and the general preference of HMGB proteins for distorted DNA, we explored the ability of HMO2 domains to bind preferentially to distorted DNA, as preferred binding might contribute to recruitment of INO80 to such structures. Furthermore, as the Box A domain of HMO2 bears little similarity to classical HMG box domains, its role in DNA binding cannot be assumed or predicted on the basis of sequence analyses.

Here we define the roles of the Box A and Box B domains of HMO2 in conferring preferred binding to various DNA substrates. As reported for mammalian HMGB proteins, the

Received: November 11, 2011
Revised: February 13, 2012
Published: February 14, 2012

acidic C-terminal extension attenuates DNA binding, thereby reducing the preference for distorted DNA structures. While both HMG domains exhibit preferred binding to distorted DNA, the unique ability of HMO2 to protect DNA ends from exonuclease-mediated digestion is conferred by the Box A domain. Consistent with the reported role of INO80 in the recovery of stalled replication forks, we further show that growth of an *hmo2*Δ strain is severely compromised upon exposure to agents that cause replication fork arrest. Combined with the preferred binding of HMO2 domains to distorted DNA, these data are consistent with a role for HMO2 in directing the INO80 complex not only to DNA ends but also to other sites of DNA damage, such as stalled replication forks.

MATERIALS AND METHODS

Cloning, Overexpression, and Purification of HMO2 Variants. Full-length HMO2 was prepared as described previously.[22] The plasmid expressing HMO2-BoxA was obtained by whole-plasmid amplification of pET14b-HMO2 carrying the gene encoding full-length HMO2 using primers that introduce a stop codon in place of threonine 81: forward primer 5′-GAAAATCTAAATAAAAAAGACACAAAG-3′ with the stop codon underlined and reverse primer 5′-GAAATG-GCTTCGTCAATAG-3′. The resulting product was transformed into *Escherichia coli* TOP10, and the construct was confirmed by sequencing. DNA encoding HMO2-BoxAB was amplified from yeast genomic DNA using forward primer 5′-CACCATGTCAGTTGAAGAAAAAAAGCG-3′, which introduces the TOPO recognition sequence (underlined), and reverse primer 5′-GATATCTTTTAATTATATATTTC-CATTTCCATCTGG-3′, which introduces a stop codon in place of lysine 158. Similarly, genes encoding HMO2-BoxB and HMO2-BoxBC were amplified from yeast genomic DNA using forward primer 5′-CACCATGCCCAAGAGGC-3′, which introduces the TOPO recognition sequence (underlined), and reverse primers 5′-GATATCTTTTAATTATATATTTC-CATTTCCATCTGG-3′ (that introduces a stop codon in place of lysine 158) and 5′-CGTCTTACCATATGTTCAAA-GAA-3′, respectively. The polymerase chain reaction (PCR) products were cloned into expression vector pET100/D-TOPO (Invitrogen), which introduces a six-histidine tag at the amino terminus.

Plasmids carrying HMO2-BoxA, HMO2-BoxAB, HMO2-BoxB, and HMO2-BoxBC were transformed into *E. coli* Rosetta Blue; expression was induced by addition of 1 mM isopropyl β-D-thiogalactopyranoside (IPTG) at an A_{600} of 0.2, and induction was conducted for 4 h at 37 °C. Cells were pelleted and resuspended in lysis buffer at pH 7.5 [50 mM $Na_xH_yPO_4$, 300 mM NaCl, 10 mM imidazole, 20% glycerol for HMO2-BoxA and 10% glycerol for HMO2-BoxB and HMO2-BoxBC, 1 mM 2-mercaptoethanol, and 1 mM phenylmethanesulfonyl fluoride (PMSF)]. Cells were disrupted by sonication, and the nucleic acids were digested by incubation with 2 μL of 2000 units/mL DNaseI (New England BioLabs) for 1 h, after which the suspension was centrifuged at 6000*g* for 20 min. For HMO2-BoxA, the cell lysate was incubated with the nickel resin for 1 h on ice and the flow-through was collected and incubated on ice for 1 h with cobalt beads previously equilibrated with lysis buffer. The nickel beads previously incubated with cleared lysates containing HMO2-BoxB and HMO2-BoxBC and the cobalt beads incubated with HMO2-BoxA were washed with wash buffer at pH 7.5 (50 mM $Na_xH_yPO_4$, 300 mM NaCl, 20 mM imidazole, 20% glycerol for HMO2-BoxA and 10% glycerol for HMO2-BoxB and HMO2-BoxBC, 1 mM 2-mercaptoethanol, and 1 mM PMSF). Proteins were eluted by gravity flow using elution buffer at pH 7.5 (50 mM $Na_xH_yPO_4$, 300 mM NaCl, 250 mM imidazole and 20% glycerol for HMO2-BoxA and 100 mM imidazole and 10% glycerol for HMO2-BoxB and HMO2-BoxBC, 1 mM 2-mercaptoethanol, and 1 mM PMSF). For HMO2-BoxAB, the cell lysate was brought to 60% ammonium sulfate. The pellet from the ammonium sulfate precipitation was dissolved and dialyzed overnight at 4 °C against HA buffer at pH 7.5 (20 mM Tris, 50 mM KCl, 10% glycerol, 1 mM 2-mercaptoethanol, and 1 mM PMSF). The dialysate was loaded onto a DEAE column, and protein was eluted with a 96 mL linear gradient from 50 mM KCl (HA buffer) to 1 M KCl. The fractions collected were dialyzed overnight at 4 °C against HA buffer at pH 6.0 and passed through CM-Sepharose, and protein was eluted with a 96 mL linear gradient from 50 mM KCl (HA buffer) to 1 M KCl. The peak fractions were pooled and dialyzed overnight at 4 °C against HA buffer at pH 7.5. The dialysate was passed through a hydroxylapatite column, and the purified protein was obtained in the flow-through. Purified proteins were quantitated using Coomassie blue-stained sodium dodecyl sulfate–polyacrylamide gel electrophoresis (SDS–PAGE) gels using bovine serum albumin as the standard.

Electrophoretic Mobility Shift Assay. Oligonucleotides were purchased (Eurofins MWG Operon) and purified by denaturing gel electrophoresis. Electrophoretic mobility shift assays (EMSAs) were performed using 50 bp DNA duplex, 50 bp DNA with two four-nucleotide loops 9 bp apart, 50 bp DNA with a single four-nucleotide loop, and 50 bp DNA with a single four-nucleotide loop separated from an abasic site by 9 bp of duplex; four-nucleotide loops were created from two consecutive mismatches of identical opposing bases and the abasic site by introducing a tetrahydofuran analogue in one DNA strand. The two identical opposing bases creating the mismatches are CT and AA. The 50 bp construct with the abasic site has a CT mismatch 9 bp upstream and an additional mismatch 7 bp upstream of the CT mismatch composed of 5′-AG-3′ in the top strand and 3′-CT-5′ in the bottom strand. Other substrates used were four-way DNA junctions, prepared as described previously,[30] and DNA with stem–loop structure.[31] For each construct, one strand was 5′-end-labeled with [γ-^{32}P]ATP using T4 polynucleotide kinase (New England BioLabs). Complementary strands were annealed by heating the samples at 90 °C and slowly cooling them to room temperature.

Reaction mixtures contained 5 fmol of DNA with varying concentrations of HMO2, HMO2-BoxA, HMO2-BoxB, or HMO2-BoxBC in 10 μL of reaction buffer [20 mM Tris (pH 8.0), 5 mM NaCl, 0.1 mM EDTA, 0.1 mM DTT, 0.1% Triton X-100, and 0.01% BRIJ58] and were incubated at room temperature for 1 h. Samples were loaded on 8% polyacrylamide gels (39:1 acrylamide:bisacrylamide) and electrophoresed using 0.5× TBE [45 mM Tris-borate (pH 8.3) and 1 mM EDTA] at 175 V for 2 h. Complexes were visualized using an Amersham Biosciences Storm Phosphorimager.

End Joining Assay. Supercoiled pGEM5 was digested with NdeI to obtain DNA with a two-nucleotide 5′-overhang. One hundred nanograms of linearized pGEM5 was incubated with varying concentrations of HMO2 or its variants at room temperature for 1 h. To this reaction mixture was added 1 μL of 400 units/μL T4 DNA ligase, and the mixture was incubated at room temperature for 1 h. Some reaction mixtures were subsequently treated with 1 μL of 100 units/μL exonuclease III

at room temperature for 1 h. Reactions were terminated using 1 μL of stop buffer (5 mM EDTA, 1.1% glycerol, and 0.2 mg/mL proteinase K). Samples were electrophoresed on 1% agarose gels in 0.5× TBE and visualized by ethidium bromide staining.

Exonuclease III Protection Assay. Supercoiled pGEM5 was linearized with NdeI and incubated at room temperature for 1 h with varying concentrations of HMO2 variants. Control reaction mixtures contained 1 μM HMO2. To each reaction mixture was added 1 μL of 100 units/μL exonuclease III, and mixtures were incubated at room temperature for 1 h. Reactions were terminated using 1 μL of 10% SDS. Samples were electrophoresed on 1% agarose gels in 0.5× TBE and visualized using ethidium bromide staining.

Yeast Strains and Knockouts. Parent yeast strain DDY3 was used.[32] A *Rad52* knockout was obtained by inactivating the *rad52* gene with kanMX. The kanMX gene was amplified from plasmid pDD777 using forward primer 5′-GGAGGTTGCCAAGAACTGCTGAAGGTTCTGGTGGCTTTGGTGTGTTGTTGGCCAGCTGAAGCTTCGTACGC-3′ and reverse primer 5′-AATAAATAATGATGCAAATTTTTTATTTGTTTCGGCCAGGAAGCGTTTCAGCATAGGCCACTAGTGGATCTG-3′. The primers are designed such that they both have a homologous region from the *rad52* gene. The PCR product was transformed into DDY3 and plated on YPD plates with kanamycin G418. The recombinant construct was identified by PCR and named SRY2. The *hmo2*Δ (DDY1301) strain was created previously,[33] and the mating type was switched to α by mating DDY1229 and DDY1301, followed by tetrad dissection to generate strain SRY1. The *hmo2* and *rad52* double knockout (SRY3) was generated by mating *rad52*Δ (SRY2) and *hmo2*Δ (SRY1), followed by tetrad dissection. The genotypes of the strains are listed in Table 1.

Table 1. Yeast Strains and Genotypes

strain	genotype	ref
DDY3	*MAT***a** *ADE2 his3-11 leu2-3,112 lys2*Δ *trp1-1 ura3-1 GAL can1-100*	32
DDY1229	*MATα ade2 his3-11 leu2-3,112 LYS2 trp1-1 ura3-1*	32
DDY1301	*MAT***a** *ADE2 his3-11 leu2-3,112 lys2*Δ *trp1-1 ura3-1 hmo2::URA3*	33
SRY1	*MATα ade2 his3-11 leu2-3,112 LYS trp1-1 ura3-1 hmo2::URA3*	this work
SRY2	*MAT***a** *ADE2 his3-11 leu2-3,112 lys2*Δ *trp1-1 ura3-1 rad52::kanMX*	this work
SRY3	*MAT***a** *ADE2 his3-11 leu2-3,112 lys2*Δ *trp1-1 ura3-1 hmo2::URA3 rad52::kanMX*	this work

Yeast Spot Dilution Assay. The yeast parent strain (DDY3) and *hmo2*Δ (SRY1), *rad52*Δ (SRY2), and *hmo2*Δ*rad52*Δ (SRY3) knockout strains were grown in liquid YPD medium to OD_{600} of 0.4 (for the exponential phase) and 1.0 (for the stationary phase). For each strain, 1, 2, 3, and 4 μL was spotted on YPD plates, YPD with 0.01% MMS (methylmethane sulfonate), YPD with 100 mM HU (hydroxyurea), and YPD with subsequent exposure to 5000 μJ of UV radiation using the Stratalinker as the UV source, respectively. Dilutions of 0, 1:10, $1:10^2$, $1:10^3$, and $1:10^6$ were used. All YPD plates were incubated at 30 °C for 2 days.

RESULTS

HMO2-BoxA and HMO2-BoxB Have a Stronger Preference for DNA with Distortions Than HMO2-BoxBC. HMO2 was previously shown to bind preferentially to supercoiled compared to linear DNA and to distorted DNA compared to perfect duplex.[22] On a 50 bp perfect duplex, HMO2 does not form complexes that are stable to electrophoresis, and DNA with tandem four-nucleotide loops was seen to be the preferred substrate compared to DNA with a single lesion, suggesting that both HMG boxes exhibit preferred binding to a DNA lesion.[22] To address the roles of the HMO2 domains in conferring such preferred binding, we created several HMO2 variants. HMO2-BoxA comprises the 81 N-terminal residues. HMO2-BoxAB is truncated for the C-terminal tail. HMO2-BoxBC is truncated for the N-terminal Box A domain. HMO2-BoxB comprises only the Box B domain from residues 91−158. HMO2-BoxAB proved to be nearly insoluble and very prone to aggregation and was not analyzed further. Purified HMO2 variants are shown in Figure S1 of the Supporting Information.

DNA binding was analyzed by an EMSA, using 50 bp DNA with tandem lesions (that is, containing a pair of four-nucleotide loops 9 bp apart). Both HMO2-BoxA and HMO2-BoxB bind to 50 bp DNA with two four-nucleotide loops and primarily form a single stable complex (Figure 1A,B), although HMO2-BoxB can form another slower migrating complex, which is not stable under electrophoresis conditions. The complex with HMO2-BoxB migrates slightly faster than that formed with HMO2-BoxA, which may be due to a difference in the modes of binding of the two domains with the DNA, such as differences in stoichiometry or DNA bend angles. HMO2-BoxBC also binds this DNA construct (Figure 1C), but the predominant complex (C1) migrates much slower than that formed with HMO2-BoxA and HMO2-BoxB. The complex formed with HMO2-BoxBC appears at lower protein concentrations but is not very stable to electrophoresis, suggesting that the negatively charged C-terminal tail significantly modulates DNA binding by Box B. That the predominant complex C1 migrates much slower than complex C2 detected at higher protein concentrations may reflect preferred association of two HMO2-BoxBC protomers on this DNA.

While full-length HMO2 binds significantly better to DNA with tandem lesions than to DNA with a single four-nucleotide loop,[22] the formation of a complex with isolated HMO2 domains is not significantly different with these DNA constructs; on DNA with a single lesion, containing the CT loop only, HMO2-BoxA, HMO2-BoxB, and HMO2-BoxBC predominantly form a single complex (Figure 1D−F) comparable to that seen with DNA with tandem lesions, except that HMO2-BoxB is more prone to forming multiple complexes (Figure 1E, complex C2), perhaps reflecting that a second lesion attenuates a protein accretion otherwise seen in its absence. These data show that both Box A and Box B domains contribute to DNA binding and suggest that the markedly enhanced binding to DNA with tandem lesions by full-length HMO2 may be due to an additive effect of each domain associating with one DNA lesion.

Only Box B Binds Preferentially to DNA with an Abasic Site. Inspired by a recent report indicating that mammalian HMGB proteins play a role in base excision repair,[34] we explored the ability of each HMO2 domain to bind DNA with an abasic site, an intermediate in this repair pathway. We used the same 50 bp DNA construct with tandem lesions, retaining the CT loop and replacing the AA loop with a single tetrahydrofuran analogue, which mimics an abasic site. The abasic site is placed 9 bp from the CT mismatch. This construct also contains another mismatch 7 bp upstream of the CT

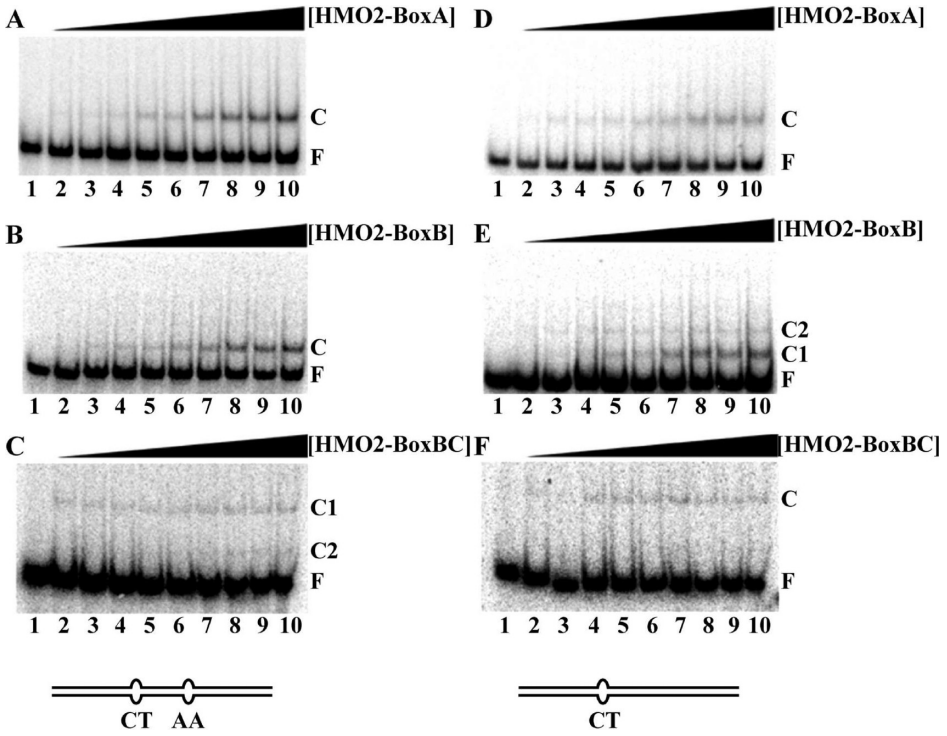

Figure 1. Interaction of HMO2 domains with DNA containing mismatches. (A–C) EMSAs with 50 bp DNA duplex with two four-nucleotide loops (composed of identical opposing AA and CT nucleotides, respectively) separated by 9 bp of duplex and increasing concentrations of indicated HMO2 variants. (A) DNA duplex with tandem four-nucleotide loops and increasing concentrations of HMO2-BoxA. (B) DNA duplex with tandem four-nucleotide loops and increasing concentrations of HMO2-BoxB. (C) DNA duplex with tandem four-nucleotide loops and increasing concentrations of HMO2-BoxBC. (D–F) EMSAs of 50 bp DNA duplex with a single four-nucleotide loop (tandem mismatches composed of opposing CT nucleotides) and increasing concentrations of HMO2 variants. (D) DNA with a single four-nucleotide loop and increasing concentrations of HMO2-BoxA. (E) DNA with a single four-nucleotide loop and increasing concentrations of HMO2-BoxB. (F) DNA with a single four-nucleotide loop and increasing concentrations of HMO2-BoxBC: lane 1, reactions with DNA only; lanes 2–10, reactions with the indicated HMO2 variant at 50, 75, 100, 250, 500, 750, 1000, 2000, and 3000 nM. Complex (C) and free DNA (F) are denoted at the right.

mismatch. EMSAs show that binding to DNA with mismatches 7 bp apart by wild-type HMO2 and HMO2-BoxB is comparable to binding to DNA with a single mismatch (data not shown).

Full-length HMO2 binds well to this DNA construct containing the abasic site 9 bp from the mismatch, forming a single complex (Figure 2A); this binding is similar to that seen with DNA containing tandem mismatches.[22] HMO2-BoxA does not form a very pronounced complex with this construct (Figure 2B); however, HMO2-BoxBC binds more stably compared to DNA with single or tandem four-nucleotide loops (Figure 2D), and HMO2-BoxB forms multiple complexes with this DNA construct (Figure 2C). For both HMO2-boxB and HMO2-BoxBC, a complex of slower mobility (C2) appears at lower protein concentrations, possibly reflecting preferred association of two protomers. It is also notable that while the presence of two four-nucleotide loops prevents accretion of additional HMO2-BoxB protomers, such association is favored on DNA containing the abasic site. Evidently, the differential DNA distortion imposed by tandem mismatches and abasic sites significantly affects the mode of binding of the HMO2 domains.

Mammalian HMGB1 was reported not only to be a cofactor in base excision repair but also to exhibit AP lyase activity.[34] Because HMO2 and HMO2-BoxB bind with significant preference to DNA with an abasic site, we tested if HMO2 has AP lyase activity. However, such activity was not detected using DNA in which an abasic site is created by uracil-DNA glycosylase (UDG)-mediated cleavage of a uracil located 9 bp from a pair of mismatches (Figure S2 of the Supporting Information).

Differential Preferences for Prebent DNA. While full-length HMO2 does bind a four-way junction in preference to a perfect duplex, the preference is modest.[22] To examine the interaction of HMO2 domains with statically deformed DNA, we chose two DNA constructs. The first is DNA with a stem–loop feature surrounded by 7 and 14 bp duplex regions (Figure 3). Full-length HMO2 binds to this DNA construct forming one predominant complex, with a second complex that can be detected at higher protein concentrations, but the migration of the complexes is much slower than that of those formed with DNA with a four-nucleotide loop and abasic site, and significant complex dissociation during electrophoresis is evident (Figure 3A). HMO2-BoxA and HMO2-BoxBC do not bind with significant preference to the stem–loop DNA (Figure 3B,D). In contrast, HMO2-BoxB forms several complexes with this DNA construct (Figure 3C), suggesting that Box B exhibits a binding preference for static DNA distortions that is abolished in the presence of the acidic tail.

For mammalian HMGB proteins, the preferred binding to four-way junction DNA is conferred by the Box A domain, and the presence of Mg^{2+}, which induces a disfavored X conformation, affects binding to the junctions.[10,13,35] For HMO2, Mg^{2+} does not affect complex formation, and binding to four-way junction DNA is only modestly preferred compared to that with the perfect duplex.[22] HMO2-BoxA forms multiple discrete complexes (Figure 4A), whereas complexes with HMO2-BoxB

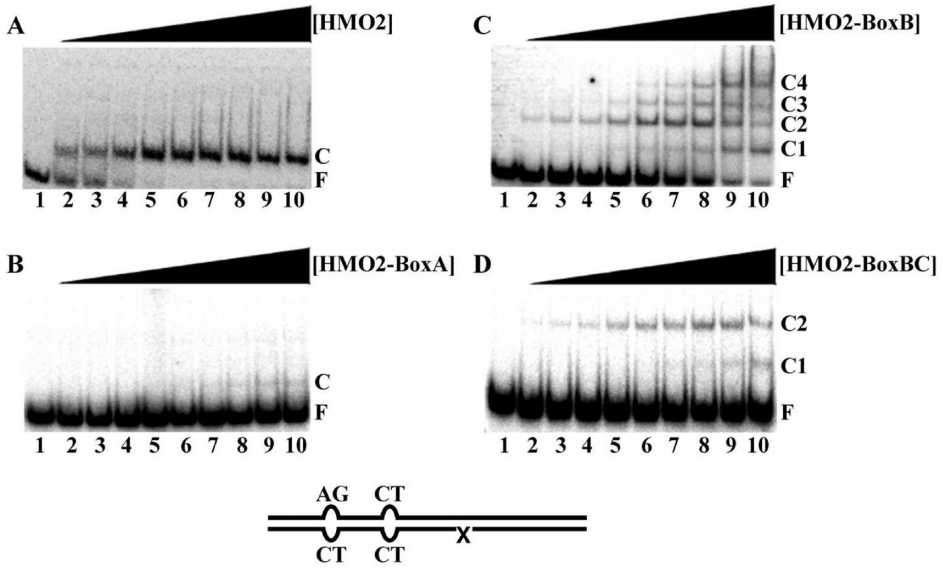

Figure 2. Interaction of HMO2 variants with DNA containing an abasic site. EMSAs with 50 bp DNA duplex with three lesions: an abasic site and a four-nucleotide loop (composed of opposing CT nucleotides) separated by 9 bp and a second four-nucleotide loop 7 bp from the four-nucleotide CT-loop. (A) HMO2, (B) HMO2-BoxA, (C) HMO2-BoxB, and (D) HMO2-BoxBC: lane 1, reactions with DNA only; lanes 2−10, reactions with the indicated HMO2 variants at 50, 75, 100, 250, 500, 750, 1000, 2000, and 3000 nM. Complex (C) and free DNA (F) are denoted at the right. In the cartoon, "X" represents the abasic (tetrahydrofuran) site.

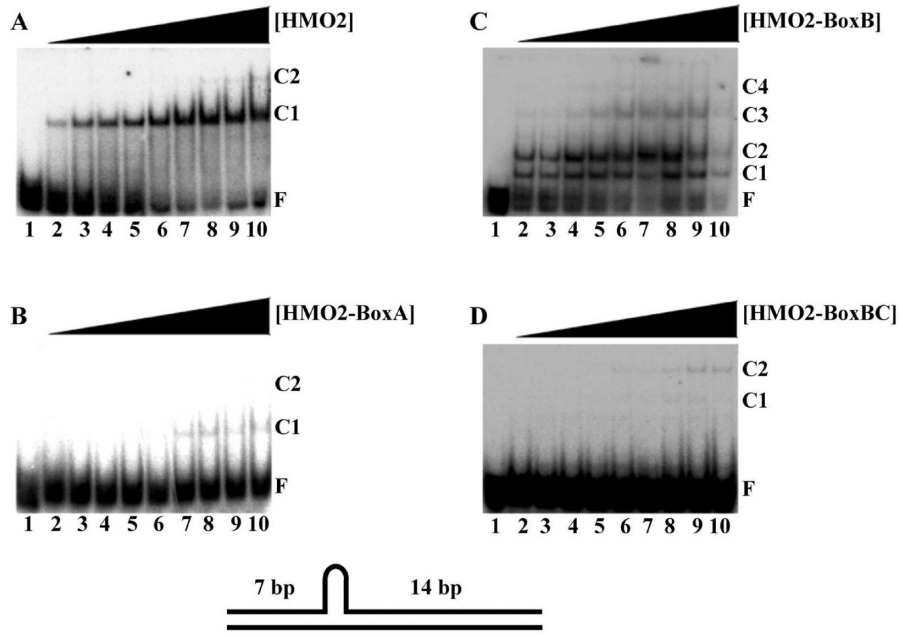

Figure 3. Interaction of HMO2 variants with stem−loop DNA. EMSAs of stem−loop DNA with increasing concentrations of the indicated HMO2 variant. (A) HMO2, (B) HMO2-BoxA, (C) HMO2-BoxB, and (D) HMO2-BoxBC: lane 1, 5 fmol of stem−loop DNA only; lanes 2−10, reactions with the indicated HMO2 variants at 50, 75, 100, 250, 500, 750, 1000, 2000, and 3000 nM, respectively. Complex (C) and free DNA (F) are denoted at the right.

dissociate during electrophoresis, although all DNA is eventually bound unlike what is observed for HMO2-BoxA at equivalent protein concentrations (Figure 4B). HMO2-BoxBC fails to form a detectable complex (Figure 4C). The presence or absence of Mg^{2+} did not have any effect on binding of the different domains to the four-way junctions (data not shown).

Box A Confers on HMO2 the Ability To Protect DNA Ends. A unique feature of full-length HMO2 is its ability to bind DNA ends and prevent DNA end joining.[22] Incubating linearized pGEM5 with low concentrations of T4 DNA ligase yields a modest level of ligated product (Figure 5A,B, lane 2). Neither HMO2-BoxA nor HMO2-BoxB enhances DNA end joining, nor do they prevent end joining at lower concentrations (Figure 5A,B, lanes 3−7, 10−100 nM). At higher protein concentrations, the disappearance of the DNA multimer indicates prevention of DNA end joining by both HMO2-BoxA and HMO2-BoxB. Treating reaction mixtures containing DNA, T4 DNA ligase, and either HMO2-BoxA or HMO2-BoxB with exonuclease III shows that HMO2-BoxA prevents DNA degradation (Figure 5A, lane 13), whereas HMO2-BoxB does not (Figure 5B, lane 14).

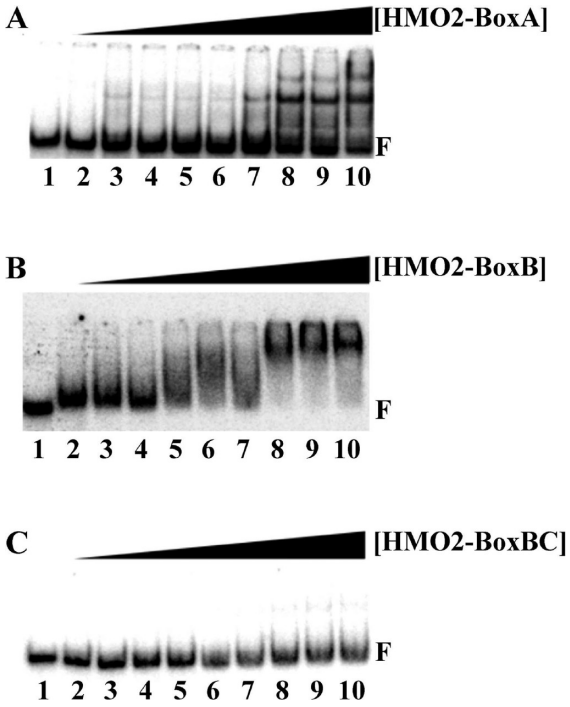

Figure 4. Binding of HMO2 domains to four-way junction DNA. EMSAs of four-way junction DNA titrated with the indicated HMO2 variant: lane 1, 5 fmol of four-way junction only; lanes 2–10, reactions with 50, 75, 100, 250, 500, 750, 1000, 2000, and 3000 nM protein, respectively. Free DNA (F) is denoted at the right.

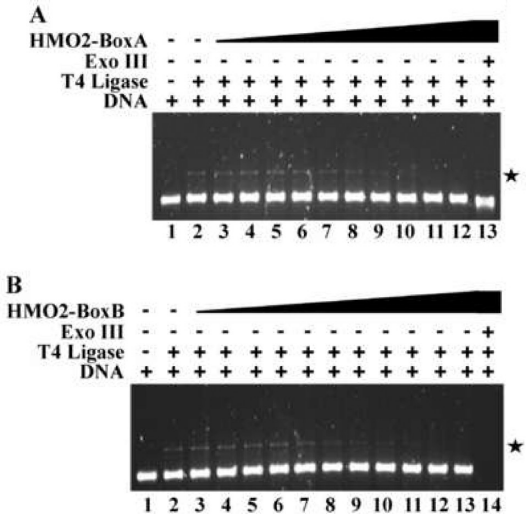

Figure 5. Ligase-mediated DNA end joining in the presence of HMO2-BoxA and HMO2-BoxB. (A) DNA with overhangs (5′-TA extensions) and increasing concentrations of HMO2-BoxA: lane 1, 100 ng of DNA (~4 nM, corresponding to ~8 nM DNA ends); lane 2, DNA and T4 DNA ligase; lanes 3–12, DNA, T4 DNA ligase, and 10, 25, 50, 75, 100, 250, 500, 750, 1000, and 2000 nM HMO2-BoxA, respectively; lane 13, DNA, T4 DNA ligase, 3000 nM HMO2-BoxA, and exonuclease III. (B) DNA with overhangs (5′-TA extensions) and increasing concentrations of HMO2-BoxB: lane 1, 100 ng of DNA; lane 2, DNA and T4 DNA ligase; lanes 3–13, DNA, T4 DNA ligase, and 10, 25, 50, 75, 100, 250, 500, 750, 1000, 2000, and 3000 nM HMO2-BoxB, respectively; lane 14, DNA, T4 DNA ligase, 3000 nM HMO2-BoxB, and exonuclease III. The ligation product is denoted with an asterisk at the right.

To determine further the ability of HMO2 domains to bind DNA ends, linearized pGEM5 was digested with exonuclease III in the presence of the various domains. HMO2-BoxA protects DNA from exonuclease III digestion at high protein concentrations [Figure 6A, lanes 4–6 (1000, 2000, and 3000 nM, respectively)]. By comparison, full-length HMO2 protects DNA ends at 1000 nM protein (Figure 6B, lane 6). In contrast, HMO2-BoxB and HMO2-BoxBC are unable to protect DNA from exonuclease III digestion (Figure 6B, lanes 4 and 5). Taken together, these data suggest that the Box A domain confers on HMO2 the ability to protect DNA ends.

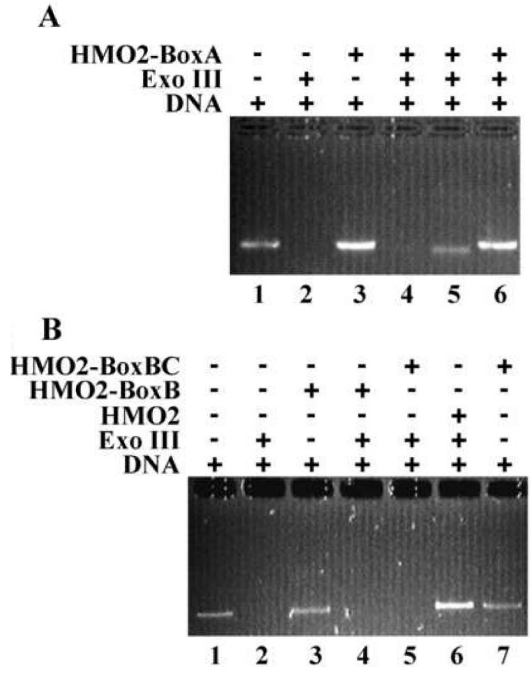

Figure 6. Exonuclease protection. (A) Lane 1, DNA only; lane 2, DNA treated with exonuclease III for 1 h; lane 3, DNA and 3000 nM HMO2-BoxA; lanes 4–6, DNA with 1000, 2000, and 3000 nM HMO2-BoxA, respectively, incubated with exonuclease III for 1 h. (B) Lane 1, DNA only; lane 2, DNA treated with exonuclease III for 1 h; lane 3, DNA with 3000 nM HMO2-BoxB; lanes 4 and 5, DNA incubated with 3000 nM HMO2-BoxB and HMO2-BoxBC, respectively, and exonuclease III for 1 h; lane 6, DNA incubated with 1000 nM HMO2 and exonuclease III for 1 h; lane 7, DNA with 3000 nM HMO2-BoxBC.

An *hmo2*Δ Strain Is Sensitive to Replication Fork Arrest. DNA end binding by HMO2 is consistent with its reported role in directing INO80 to DSBs.[19,20] INO80 is also enriched at stalled replication forks, where it is required for replication to resume after recovery from fork arrest.[23,36] Stalled forks may eventually collapse, yielding DNA breaks that must be repaired by homologous recombination. Since HMO2 was reported to be required for recruitment of yeast INO80 to DNA DSBs, it may also be required for recruitment of this chromatin remodeling complex to stalled replication forks; the latter should yield an increased sensitivity in an *hmo2*Δ strain to agents such as hydroxyurea (HU) that cause replication fork arrest. To address this hypothesis, we inactivated the *hmo2* and *rad52* genes by insertion of *URA3* and *KanMX* marker genes, respectively, and mated *hmo2*Δ and *rad52*Δ to produce an *hmo2*Δ*rad52*Δ double knockout strain.

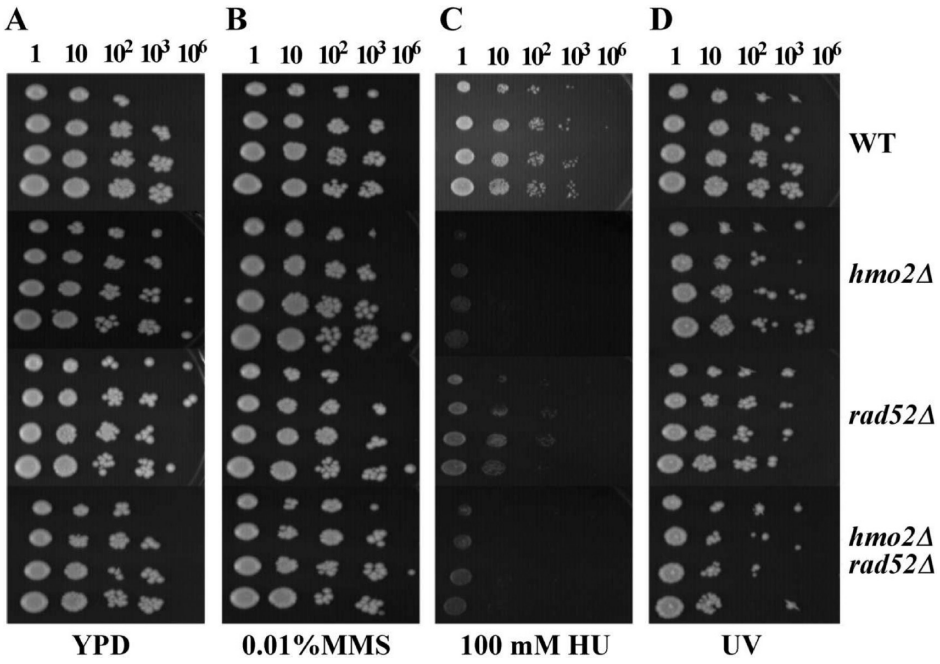

Figure 7. Growth comparison of wild-type and knockout yeast in the exponential phase in the presence of different DNA-damaging agents. (A) Growth of wild-type, *hmo2*Δ, *rad52*Δ, and *hmo2*Δ*rad52*Δ yeast on YPD media. (B) Growth of wild-type, *hmo2*Δ, *rad52*Δ, and *hmo2*Δ*rad52*Δ yeast on YPD media with 0.01% methylmethane sulfonate (MMS). (C) Growth of wild-type, *hmo2*Δ, *rad52*Δ, and *hmo2*Δ*rad52*Δ yeast on YPD media with 100 mM hydroxyurea (HU). (D) Growth of wild-type, *hmo2*Δ, *rad52*Δ, and *hmo2*Δ*rad52*Δ yeast on YPD media following exposure to UV radiation. All plates were incubated at 30 °C for 2 days.

Figure 7 shows the sensitivity of exponentially growing wild-type and knockout strains to the alkylating agent methylmethane sulfonate (MMS), HU, and UV radiation compared to cells grown on YPD media without any exposure to a DNA-damaging agent. In the absence of induced DNA damage, no obvious growth phenotype is associated with either gene deletion, and no difference is evident upon exposure to MMS either. In contrast, a significant difference was observed upon exposure to HU; the *hmo2*Δ strain is more sensitive than the *rad52*Δ strain, and the growth phenotype of the *hmo2*Δ*rad52*Δ strain is comparable to that of the *hmo2*Δ strain. When the four strains were irradiated with UV, *hmo2*Δ and *rad52*Δ strains exhibit modestly slower growth than the wild type, with the most severe growth phenotype seen for the *hmo2*Δ*rad52*Δ strain. Similar sensitivity patterns for the four strains were observed at the stationary phase as indicated in Figure S4 of the Supporting Information. The observed severe phenotype of the *hmo2*Δ strain associated with exposure to HU is consistent with a role for HMO2 in recruiting INO80 not only to DSBs but also to stalled replication forks.

DISCUSSION

The Acidic C-Terminal Tail Attenuates DNA Binding. HMO2 binds preferentially to 50 bp DNA with pairs of tandem mismatches compared to DNA with a single lesion, suggesting that both Box A and Box B domains exhibit preferred binding to such lesions.[22] Consistent with this interpretation, we found that both HMO2-BoxA and HMO2-BoxB bind comparably to DNA with one or two sets of mismatches (Figure 1). What is also worth emphasizing is that the Box A domain, despite its limited sequence similarity to consensus HMG boxes, does participate in DNA binding. In contrast, HMO2-BoxBC binds poorly, indicating that the negatively charged C-terminal tail attenuates DNA binding by Box B.

It has been reported for mammalian HMGB1 that the C-terminal tail reduces DNA binding in vitro and also weakens preferences for bent DNA;[37,38] the acidic tail binds intramolecularly to the DNA-binding face of both HMG boxes, Box B in particular, thus attenuating DNA binding.[39,40] Fragments of calf thymus HMGB1 obtained by protease V8 cleavage have also been analyzed, and the fragment corresponding to Box B and the C-terminal tail was found to have lost secondary structure content as well as the ability to constrain DNA supercoiling.[41] The inference from this work is that the C-terminal tail interacts more strongly with Box B when Box A is absent, in the process disrupting secondary structure. Consistent with this interpretation, the N- and C-terminal extensions of maize HMGB1 were shown to interact; deletion of the Box A domain and the basic N-terminal extension might therefore result in interactions between the C-terminal tail and Box B that would otherwise not occur in the full-length protein.[42] By contrast, it has also been suggested, on the basis of differential scanning calorimetry and circular dichroism spectroscopy of recombinant HMGB1 fragments, that the HMG domain that interacts with the C-terminal tail in the context of the full-length protein is stabilized by this interaction.[43] For yeast HMO1, interactions between its C-terminal tail and the Box A domain have been reported and inferred to be destabilizing; however, in HMO1, the C-terminal tail is lysine-rich.[14] Taken together, interactions between Box B and the C-terminal tail of mammalian HMGB1 are well-established, and such interactions have been shown to regulate DNA binding negatively. Considering that binding of DNA by HMO2-BoxBC is attenuated but not abolished (e.g., Figures 1 and 2), we surmise that HMO2-BoxBC either retains its folded structure or folds upon DNA binding, unlike what has been reported for mammalian HMGB1-BoxBC fragments.[41] The weakened DNA binding by HMO2-BoxBC, however, is consistent with published reports on mammalian HMGB1.

dx.doi.org/10.1021/bi201700h | *Biochemistry* 2012, 51, 1825−1835

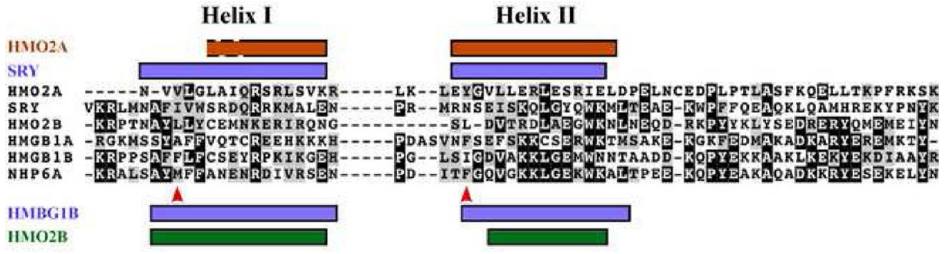

Figure 8. Sequence alignment of HMG domains: rat HMGB1-BoxA (HMGBA) and HMGB1-BoxB (HMGBB), human SRY, yeast NHP6a, HMO2-BoxA (HMO2A), and HMO2-BoxB (HMO2B). Helical segments from SRY are identified above the alignment (blue), with helical segments from rat HMGB1-BoxB identified below the alignment.[11] The intercalating residues in helices I and II are highlighted with red arrowheads. The sequence alignment was generated using MUSCLE.[54] HMO2 was modeled using ESyPred3D[53] with the SRY B didomain (Protein Data Bank entry 2GZK) as a template;[11] predicted helical segments of HMO2-BoxA (modeled on the SRY component of the SRY.B didomain) are colored orange, and those of HMO2-BoxB (modeled on the Box B component of SRY.B) are colored green. For HMO2-BoxA, the modeling did not include sequence upstream of the conserved R in helix I; possible extension of helix I is indicated by the hatched outline.

The acidic C-terminal tail of mammalian HMGB1 has also been shown to interact with the N-terminus of histone H3, an interaction that likely participates in directing HMGB1 to chromatin.[44] The acidic tail also contacts the basic C-terminal domain of linker histone H1; when this occurs, its interaction with the DNA-binding faces of the HMG boxes is disrupted, perhaps leading to preferred binding of the HMGB protein to the linker DNA and displacement of H1.[45] Similarly, it is possible that the acidic tail of HMO2 mediates its recruitment to chromatin. Further, because neither HMO2-BoxB nor HMO2-BoxBC binds well to perfect duplex DNA and because DNA lesions mainly enhance binding by HMO2-BoxB, the C-terminal extension of HMO2 also appears to attenuate the preference for DNA distortions.

HMO2-BoxA and HMO2-BoxB Exhibit a Differential Preference for Distorted DNA. For mammalian HMGB1, it is the Box A domain that confers preferred binding to distorted DNA.[10,46] For HMO2, both domains bind with marked but differential preference to distorted DNA structures, with HMO2-BoxB binding DNA with a wider range of lesions compared to HMO2-BoxA, which primarily binds DNA with tandem mismatches and four-way junctions (Figures 3 and 4). There is also a difference in the migration of complexes with the HMO2 variants and 50 bp DNA with tandem mismatches. Complexes with HMO2-BoxA migrate somewhat slower than those with HMO2-BoxB (compare panels A and D of Figure 1 with panels B and E); this could be due to the stoichiometry with which the two HMO2 variants interact with the DNA, or it could be due to differential DNA bending by the two proteins. The pI of the domains would also be expected to affect migration of the complexes; the calculated pI values are 9.2, 6.25, and 4.8 for the Box A domain, the Box B domain, and the Box BC domain, respectively. Differences in pI may therefore contribute to the slower migration of complexes with HMO2-BoxA compared to HMO2-BoxB, whereas the slower migration of complexes with HMO2-BoxBC is more likely due to the stoichiometry with which HMO2-BoxBC interacts with the DNA. When HMO2-BoxBC binds DNA with an abasic site and DNA with a pair of tandem mismatches, a faster-migrating complex is seen only at higher protein concentrations. On these DNA constructs, the presence of the acidic tail therefore appears to promote protein−protein interaction.

DNA with mismatches is destabilized relative to perfect duplex, but the extent of destabilization depends on the nature of the mismatch and the sequence context in which it occurs. Such conformational flexibility typically promotes binding by DNA-bending proteins.[47] Intrinsic flexibility is a result of rapid interconversion between energetically comparable structures, some of which may be captured on protein binding. Binding to distinct DNA lesions can therefore likely be attributed to both different distributions of structures in solution and the extent to which existing structures are amenable to protein-mediated bending. DNA with abasic sites is likewise destabilized in a sequence context-dependent fashion. Despite the thermodynamic destabilization, such DNA usually adopts a largely *B*-form conformation, and duplex structures determined using tetrahydrofuran residues are likewise nearly B-form with the lesion in an intrahelical conformation.[48−50] However, the calculation of the energetic cost associated with DNA bending by DNA containing various lesions suggests that abasic sites may be compatible with multiple conformations in which a bend occurs in different directions,[51] a conformational flexibility that may form the basis for the preferred binding by HMO2-BoxB compared to DNA with tandem mismatches.

HMGB proteins generally bind preferentially to four-way junctions.[10,13,35] Full-length HMO2 has an only modest preference for these DNA constructs,[22] but HMO2-BoxA forms several complexes with the four-way junctions (Figure 4A); complexes with HMO2-BoxB are less discrete (Figure 4B). Because addition of the lysine-rich tail completely prevents DNA binding by HMO2-BoxBC (Figure 4C), residual binding to four-way junctions by full-length HMO2 is likely due to the Box A domain. For mammalian HMGB proteins, Box A has also been shown to confer a preference for four-way junctions, a preference in part associated with an intercalating residue in helix II.[10,46] For each of the HMG boxes of mammalian HMGB1, both helices I and II may feature hydrophobic residues that contribute to DNA binding affinity by partial intercalation between DNA bases. For the Box A domain, the intercalating residue is in helix II (Figure 8), whereas the Box B domain features potential intercalating residues in both helices. The Box B domain therefore introduces a larger bend, while Box A has a stronger preference for distorted DNA because of stacking of its helix II bending wedge on an exposed base pair.[10,46,52] Box A and Box B also differ with regard to the shape and orientation of helix I, which is short and straight in Box A and bent in Box B; DNA binding therefore also depends on the global fold of the HMG box and its complementarity to the shape of the DNA.[7]

A sequence alignment of mammalian HMGB1-BoxA, HMGB1-BoxB, and SRY with yeast NHP6A and the Box A and Box B domains of HMO2 indicates the confirmed or predicted hydrophobic intercalating residues (Figure 8). For

the sequence specific SRY, no hydrophobic residue is present in helix II, while the single HMG-Box protein NHP6A features hydrophobic residues in both helices I and II. The sequence of HMO2-BoxB aligns well with that of mammalian Box B; this alignment is also corroborated by modeling of HMO2 based on the structure of the SRY.B didomain, a structure in which SRY fused to mammalian Box B is bound to DNA.[11,53] HMO2-BoxB is predicted to feature a leucine in the position corresponding to the intercalating phenylalanine in helix I of mammalian Box B as well as a leucine in the loop preceding helix II, in a position comparable to that of the intercalating isoleucine in helix II of mammalian Box B (Figure 8 and Figure S3 of the Supporting Information). In the HMO2 model, Box A and Box B are in a head-to-head orientation, with Box A displaced slightly upstream relative to SRY (Figure S3 of the Supporting Information). According to the model, a tyrosine at the beginning of helix II corresponds to the asparagine of SRY; however, the model includes only sequence downstream of the conserved arginine in helix I, and a valine is predicted at the position of the intercalating residue in helix I solely on the basis of sequence alignments (Figure 8). Thus, both Box A and Box B domains are predicted to feature residues capable of DNA intercalation, consistent with preferred binding to distorted DNA structures. That structure-based modeling does not predict a helix I for the Box A domain that is comparable to that seen in existing HMG structures may indicate structural divergence. Considering that the Box A domain confers on HMO2 the unusual ability to protect DNA ends from exonuclease III digestion, such structural divergence may contribute to a unique preference for DNA ends.

HMO2 May Direct INO80 to Sites of DNA Damage. The chromatin remodeling complex INO80 contains the Ino80 ATPase, which belongs to the SNF/SWI2 superfamily. INO80 functions in several DNA repair pathways, including DSB repair and nucleotide excision repair, and it has been shown to participate in the restart of DNA replication following replication stress.[18−21,23−26] Replication forks may stall when they encounter DNA damage, and their regress can lead to the formation of unusual DNA structures. Stalled forks may also collapse, which leads to DSBs and recruitment of the homologous recombination repair machinery. The key role of INO80 in recovery of stalled forks is reflected in the observation that the absence of Ino80 leads stalled forks to collapse, and prolonged exposure to hydroxyurea (HU), which causes replication fork arrest, is lethal.[23,24] The function of INO80 in NER-mediated repair of UV lesions is reflected in a moderate sensitivity to UV light upon inactivation of *ino80*.[25,26]

The role of HMO2 in delivering yeast INO80 to DSBs has been reported, and this event depends on the damage-dependent phosphorylation of histone H2A on serine 129 to generate γ-H2AX.[19,20] Replication stress has been likewise associated with the generation of γ-H2AX.[27] While DSBs are for instance generated by ionizing radiation or by collapse of stalled replication forks, exposure to UV primarily produces cross-linked pyrimidine dimers that must be repaired by nucleotide excision repair (NER). Such UV damage also leads to the generation of γ-H2AX.[28,29] Upon inactivation of *hmo2*, we observe a growth phenotype that mimics that observed upon inactivation of *ino80*, namely a modest growth inhibition on exposure to UV light and a severe growth phenotype associated with replication fork arrest. Considering that HMO2 is essential for recruitment of INO80 to DSB sites in a γ-H2AX-dependent fashion, the growth phenotypes associated with UV exposure or replication fork arrest are consistent with HMO2 being likewise required for recruitment of INO80 to stalled forks and UV lesions. The DNA binding properties of HMO2, preferred binding to DNA ends and DNA lesions and static bends, are consistent with such function.

■ ASSOCIATED CONTENT

Supporting Information

A schematic representation of the HMO2 domain structure as well as SDS−PAGE gels documenting the purity of the protein preparations (Figure S1), evidence that HMO2 does not exhibit AP lyase activity (Figure S2), a structure-based model of HMO2-BoxA and -BoxB with predicted DNA-intercalating residues highlighted (Figure S3), and growth of yeast wild-type and knockout strains after exposure to DNA-damaging agents in the stationary phase (Figure S4), where the results are equivalent to those obtained when DNA damage is induced in the exponential phase (Figure 7). This material is available free of charge via the Internet at http://pubs.acs.org.

■ AUTHOR INFORMATION

Corresponding Author

*Department of Biological Sciences, Louisiana State University, Baton Rouge, LA 70803. Telephone: (225) 578-5148. E-mail: agrove@lsu.edu.

Present Address

†Molecular Carcinogenesis, University of Texas M. D. Anderson Cancer Center, Smithville, TX 78957.

Funding

Supported by National Science Foundation Grants MCB-0744240 and MCB-1051610 to A.G.

Notes

The authors declare no competing financial interest.

■ ACKNOWLEDGMENTS

We are grateful to D. Donze for helpful advice with yeast genetics and for many insightful discussions.

■ ABBREVIATIONS

DSB, double-strand break; EMSA, electrophoretic mobility shift assay; HMG, high mobility group; HU, hydroxyurea; MMS, methylmethane sulfonate; PMSF, phenylmethanesulfonyl fluoride.

■ REFERENCES

(1) Bustin, M. (1999) Regulation of DNA-dependent activities by the functional motifs of the high-mobility-group chromosomal proteins. *Mol. Cell. Biol. 19*, 5237−5246.

(2) Lange, S. S., Mitchell, D. L., and Vasquez, K. M. (2008) High mobility group protein B1 enhances DNA repair and chromatin modification after DNA damage. *Proc. Natl. Acad. Sci. U.S.A. 105*, 10320−10325.

(3) Giavara, S., Kosmidou, E., Hande, M. P., Bianchi, M. E., Morgan, A., d'Adda di Fagagna, F., and Jackson, S. P. (2005) Yeast Nhp6A/B and mammalian Hmgb1 facilitate the maintenance of genome stability. *Curr. Biol. 15*, 68−72.

(4) Das, D., and Scovell, W. M. (2001) The binding interaction of HMG-1 with the TATA-binding protein/TATA complex. *J. Biol. Chem. 276*, 32597−32605.

(5) Moreira, J. M., and Holmberg, S. (2000) Chromatin-mediated transcriptional regulation by the yeast architectural factors NHP6A and NHP6B. *EMBO J. 19*, 6804−6813.

(6) Thomas, J. O. (2001) HMG1 and 2: architectural DNA-binding proteins. *Biochem. Soc. Trans. 29*, 395−401.
(7) Klass, J., Murphy, F. V. IV, Fouts, S., Serenil, M., Changela, A., Siple, J., and Churchill, M. E. (2003) The role of intercalating residues in chromosomal high-mobility-group protein DNA binding, bending and specificity. *Nucleic Acids Res. 31*, 2852−2864.
(8) Allain, F. H., Yen, Y. M., Masse, J. E., Schultze, P., Dieckmann, T., Johnson, R. C., and Feigon, J. (1999) Solution structure of the HMG protein NHP6A and its interaction with DNA reveals the structural determinants for non-sequence-specific binding. *EMBO J. 18*, 2563−2579.
(9) Weir, H. M., Kraulis, P. J., Hill, C. S., Raine, A. R., Laue, E. D., and Thomas, J. O. (1993) Structure of the HMG box motif in the B-domain of HMG1. *EMBO J. 12*, 1311−1319.
(10) Webb, M., and Thomas, J. O. (1999) Structure-specific binding of the two tandem HMG boxes of HMG1 to four-way junction DNA is mediated by the A domain. *J. Mol. Biol. 294*, 373−387.
(11) Stott, K., Tang, G. S., Lee, K. B., and Thomas, J. O. (2006) Structure of a complex of tandem HMG boxes and DNA. *J. Mol. Biol. 360*, 90−104.
(12) Ohndorf, U. M., Rould, M. A., He, Q., Pabo, C. O., and Lippard, S. J. (1999) Basis for recognition of cisplatin-modified DNA by high-mobility-group proteins. *Nature 399*, 708−712.
(13) Pöhler, J. R., Norman, D. G., Bramham, J., Bianchi, M. E., and Lilley, D. M. (1998) HMG box proteins bind to four-way DNA junctions in their open conformation. *EMBO J. 17*, 817−826.
(14) Bauerle, K. T., Kamau, E., and Grove, A. (2006) Interactions between N- and C-terminal domains of the *Saccharomyces cerevisiae* high-mobility group protein HMO1 are required for DNA bending. *Biochemistry 45*, 3635−3645.
(15) Kamau, E., Bauerle, K. T., and Grove, A. (2004) The *Saccharomyces cerevisiae* high mobility group box protein HMO1 contains two functional DNA binding domains. *J. Biol. Chem. 279*, 55234−55240.
(16) Xiao, L., Williams, A. M., and Grove, A. (2010) The C-terminal domain of yeast high mobility group protein HMO1 mediates lateral protein accretion and in-phase DNA bending. *Biochemistry 49*, 4051−4059.
(17) Xiao, L., and Grove, A. (2009) Coordination of Ribosomal Protein and Ribosomal RNA Gene Expression in Response to TOR Signaling. *Curr. Genomics 10*, 198−205.
(18) Shen, X., Mizuguchi, G., Hamiche, A., and Wu, C. (2000) A chromatin remodelling complex involved in transcription and DNA processing. *Nature 406*, 541−544.
(19) Morrison, A. J., Highland, J., Krogan, N. J., Arbel-Eden, A., Greenblatt, J. F., Haber, J. E., and Shen, X. (2004) INO80 and γ-H2AX interaction links ATP-dependent chromatin remodeling to DNA damage repair. *Cell 119*, 767−775.
(20) van Attikum, H., Fritsch, O., Hohn, B., and Gasser, S. M. (2004) Recruitment of the INO80 complex by H2A phosphorylation links ATP-dependent chromatin remodeling with DNA double-strand break repair. *Cell 119*, 777−788.
(21) Au, T. J., Rodriguez, J., Vincent, J. A., and Tsukiyama, T. (2011) ATP-dependent chromatin remodeling factors tune S phase checkpoint activity. *Mol. Cell. Biol. 31*, 4454−4463.
(22) Ray, S., and Grove, A. (2009) The yeast high mobility group protein HMO2, a subunit of the chromatin-remodeling complex INO80, binds DNA ends. *Nucleic Acids Res. 37*, 6389−6399.
(23) Papamichos-Chronakis, M., and Peterson, C. L. (2008) The Ino80 chromatin-remodeling enzyme regulates replisome function and stability. *Nat. Struct. Mol. Biol. 15*, 338−345.
(24) Shimada, K., Oma, Y., Schleker, T., Kugou, K., Ohta, K., Harata, M., and Gasser, S. M. (2008) Ino80 chromatin remodeling complex promotes recovery of stalled replication forks. *Curr. Biol. 18*, 566−575.
(25) Jiang, Y., Wang, X., Bao, S., Guo, R., Johnson, D. G., Shen, X., and Li, L. (2010) INO80 chromatin remodeling complex promotes the removal of UV lesions by the nucleotide excision repair pathway. *Proc. Natl. Acad. Sci. U.S.A. 107*, 17274−17279.
(26) Sarkar, S., Kiely, R., and McHugh, P. J. (2010) The Ino80 chromatin-remodeling complex restores chromatin structure during UV DNA damage repair. *J. Cell Biol. 191*, 1061−1068.
(27) Ward, I. M., and Chen, J. (2001) Histone H2AX is phosphorylated in an ATR-dependent manner in response to replicational stress. *J. Biol. Chem. 276*, 47759−47762.
(28) Limoli, C. L., Giedzinski, E., Bonner, W. M., and Cleaver, J. E. (2002) UV-induced replication arrest in the xeroderma pigmentosum variant leads to DNA double-strand breaks, γ-H2AX formation, and Mre11 relocalization. *Proc. Natl. Acad. Sci. U.S.A. 99*, 233−238.
(29) Oh, K. S., Bustin, M., Mazur, S. J., Appella, E., and Kraemer, K. H. (2011) UV-induced histone H2AX phosphorylation and DNA damage related proteins accumulate and persist in nucleotide excision repair-deficient XP-B cells. *DNA Repair 10*, 5−15.
(30) Ghosh, S., and Grove, A. (2004) Histone-like protein HU from *Deinococcus radiodurans* binds preferentially to four-way DNA junctions. *J. Mol. Biol. 337*, 561−571.
(31) Andrews, B. J., Lehman, J. A., and Turchi, J. J. (2006) Kinetic analysis of the Ku-DNA binding activity reveals a redox-dependent alteration in protein structure that stimulates dissociation of the Ku-DNA complex. *J. Biol. Chem. 281*, 13596−13603.
(32) Simms, T. A., Dugas, S. L., Gremillion, J. C., Ibos, M. E., Dandurand, M. N., Toliver, T. T., Edwards, D. J., and Donze, D. (2004) TFIIIC binding sites function as both heterochromatin barriers and chromatin insulators in *Saccharomyces cerevisiae*. *Eukaryotic Cell 7*, 2078−2086.
(33) Kamau, E. (2004) DNA Supercoiling with a Twist. Ph.D. Dissertation, Louisiana State University, Baton Rouge, LA.
(34) Prasad, R., Liu, Y., Deterding, L. J., Poltoratsky, V. P., Kedar, P. S., Horton, J. K., Kanno, S., Asagoshi, K., Hou, E. W., Khodyreva, S. N., Lavrik, O. I., Tomer, K. B., Yasui, A., and Wilson, S. H. (2007) HMGB1 is a cofactor in mammalian base excision repair. *Mol. Cell 27*, 829−841.
(35) Ferrari, S., Harley, V. R., Pontiggia, A., Goodfellow, P. N., Lovell-Badge, R., and Bianchi, M. E. (1992) SRY, like HMG1, recognizes sharp angles in DNA. *EMBO J. 11*, 4497−4506.
(36) Vincent, J. A., Kwong, T. J., and Tsukiyama, T. (2008) ATP-dependent chromatin remodeling shapes the DNA replication landscape. *Nat. Struct. Mol. Biol. 15*, 477−484.
(37) Wang, Q., Zeng, M., Wang, W., and Tang, J. (2007) The HMGB1 acidic tail regulates HMGB1 DNA binding specificity by a unique mechanism. *Biochem. Biophys. Res. Commun. 360*, 14−19.
(38) Stros, M., Stokrova, J., and Thomas, J. O. (1994) DNA looping by the HMG-box domains of HMG1 and modulation of DNA binding by the acidic C-terminal domain. *Nucleic Acids Res. 22*, 1044−1051.
(39) Stott, K., Watson, M., Howe, F. S., Grossmann, J. G., and Thomas, J. O. (2010) Tail-mediated collapse of HMGB1 is dynamic and occurs via differential binding of the acidic tail to the A and B domains. *J. Mol. Biol. 403*, 706−722.
(40) Knapp, S., Müller, S., Digilio, G., Bonaldi, T., Bianchi, M. E., and Musco, G. (2004) The long acidic tail of high mobility group box 1 (HMGB1) protein forms an extended and flexible structure that interacts with specific residues within and between the HMG boxes. *Biochemistry 43*, 11992−11997.
(41) Carballo, M., Puigdomènech, P., Tancredi, T., and Palau, J. (1984) Interaction between domains in chromosomal protein HMG-1. *EMBO J. 3*, 1255−1261.
(42) Thomsen, M. S., Franssen, L., Launholt, D., Fojan, P., and Grasser, K. D. (2004) Interactions of the basic N-terminal and the acidic C-terminal domains of the maize chromosomal HMGB1 protein. *Biochemistry 43*, 8029−8037.
(43) Ramstein, J., Locker, D., Bianchi, M. E., and Leng, M. (1999) Domain-domain interactions in high mobility group 1 protein (HMG1). *Eur. J. Biochem. 260*, 692−700.
(44) Ueda, T., Chou, H., Kawase, T., Shirakawa, H., and Yoshida, M. (2004) Acidic C-tail of HMGB1 is required for its target binding to nucleosome linker DNA and transcription stimulation. *Biochemistry 43*, 9901−9908.

(45) Cato, L., Stott, K., Watson, M., and Thomas, J. O. (2008) The interaction of HMGB1 and linker histones occurs through their acidic and basic tails. *J. Mol. Biol. 384*, 1262−1272.
(46) Teo, S. H., Grasser, K. D., and Thomas, J. O. (1995) Differences in the DNA-binding properties of the HMG-box domains of HMG1 and the sex-determining factor SRY. *Eur. J. Biochem. 230*, 943−950.
(47) Grove, A., Galeone, A., Mayol, L., and Geiduschek, E. P. (1996) Localized DNA flexibility contributes to target site selection by DNA-bending proteins. *J. Mol. Biol. 260*, 120−125.
(48) Kalnik, M. W., Kouchakdjian, M., Li, B. F., Swann, P. F., and Patel, D. J. (1988) Base pair mismatches and carcinogen-modified bases in DNA: An NMR study of G·T and G·O4meT pairing in dodecanucleotide duplexes. *Biochemistry 27*, 108−115.
(49) Cuniasse, P., Fazakerley, G. V., Guschlbauer, W., Kaplan, B. E., and Sowers, L. C. (1990) The abasic site as a challenge to DNA polymerase. A nuclear magnetic resonance study of G, C and T opposite a model abasic site. *J. Mol. Biol. 213*, 303−314.
(50) de Los Santos, C., El-Khateeb, M., Rege, P., Tian, K., and Johnson, F. (2004) Impact of the C1′ configuration of abasic sites on DNA duplex structure. *Biochemistry 43*, 15349−15357.
(51) Curuksu, J., Zakrzewska, K., and Zacharias, M. (2008) Magnitude and direction of DNA bending induced by screw-axis orientation: influence of sequence, mismatches and abasic sites. *Nucleic Acids Res. 36*, 2268−2283.
(52) Paull, T. T., Haykinson, M. J., and Johnson, R. C. (1993) The nonspecific DNA-binding and -bending proteins HMG1 and HMG2 promote the assembly of complex nucleoprotein structures. *Genes Dev. 7*, 1521−1534.
(53) Lambert, C., Leonard, N., De Bolle, X., and Depiereux, E. (2002) ESyPred3D: Prediction of proteins 3D structures. *Bioinformatics 18*, 1250−1256.
(54) Edgar, R. C. (2004) MUSCLE: Multiple sequence alignment with high accuracy and high throughput. *Nucleic Acids Res. 32*, 1792−1797.